First-Order Coulomb-Modified Eikonal Model Analysis for ^{16}O Ion Elastic Scatterings at E_{lab} = 1503 MeV and Tangential Velocity Correction

Yong Joo Kim

Department of Physics, Cheju National University, Jeju 690-756

The elastic scatterings of ^{16}O + ^{40}Ca and ^{16}O + ^{90}Zr systems at E_{lab} = 1503 MeV have been analyzed within the framework of the first-order Coulomb-modified eikonal model based on the tangential velocity at the distance of closest approach. The differential and reaction cross sections calculated from tangential velocity improve the agreements with the experimental data and optical model results compared to the calculated results from asymptotic velocity. Through near- and far-side decompositions of the elastic cross section, we have shown that the oscillations of the ^{16}O + ^{40}Ca system are due to the strong interference between the near- and far-side amplitudes, and the near-side one dominates for the ^{16}O + ^{90}Zr system.

I. INTROCUCTION

Heavy-ion elastic scattering studies are the most direct and simplest approach to the nucleus-nucleus interaction. The interpretation and description of scattering phenomena in heavy-ion reactions have been greatly facilitated by the application of semiclassical methods. The one method for semiclassical analysis of elastic scattering data is the eikonal approximation [1-5]. In general, the eikonal phase shift is derived from the integral equation by further approximating the WKB results [1,2]. Over the years the eikonal approximation has been a useful tool to describe the heavy-ions elastic scattering. There has been a great deal of efforts [5-10] in describing scattering processes between heavy-ions within the framework of the eikonal approximation method. The Glauber model with first- and second-order non-eikonal corrections has been applied to elastic nuclear scattering at intermediate energies by Fäldt *et al.* [6]. The first- and third-order non-eikonal corrections to the Glauber model have been developed to know the possibility of observing a bright interior in the nucleus "viewed" by intermediate energy alpha particles (E_α=172.5 MeV), as a probe for the ^{58}Ni nucleus [9]. Aguiar *et al.* [10] have discussed different schemes devised to extend the eikonal approximation to the regime of low bombarding energies in heavy-ion collisions.

Cha and Kim [11] have presented the first- and second-order corrections to the zeroth-order eikonal phase shifts for heavy-ion elastic scatterings based on Coulomb trajectories of colliding nuclei and it has been applied satisfactorily to the ^{16}O + ^{40}Ca and ^{16}O + ^{90}Zr systems at E_{lab}=1503 MeV. The refractive elastic scatterings of ^{12}C + ^{12}C system at E_{lab}=240, 360 and 1016 MeV are analyzed within a framework of a first-order Coulomb-modified eikonal model [12]. Roussel-Chomaz *et al.* [13] have measured the elastic scattering of ^{16}O + ^{40}Ca and ^{16}O + ^{90}Zr systems at E_{lab} = 1503 MeV, and analyzed it using the optical model. It is interesting to extend the fisrt-order Coulomb-modified eikonal model formalism to take into account the tangential velocity at turning point of the corresponding classical trajectory and apply it to the elastic ^{16}O + ^{40}Ca and ^{16}O + ^{90}Zr scatterings at E_{lab} = 1503 MeV. In this study, we maintain the first-order Coulomb-modified eikonal form of the phase shift and try to replace the asymptotic velocity by tangential velocity at the point of closest approach. In section II, we present the theory related with the first-order eikonal formalism based on Coulomb trajectories and its tangential velocity at the turning point. Section III contains results and discussions. Finally, concluding remarks are presented in section IV.

II. THEORY

The elastic scattering amplitude $f(\theta)$ for spin-zero particles via Coulomb and short-

range central forces is given by the equation

$$f(\theta) = f_{\mathrm{R}}(\theta) + \frac{1}{ik}\sum_{L=0}^{\infty}(L + \frac{1}{2})\exp(2i\sigma_L)$$
$$\times(S_L^{\mathrm{N}} - 1)P_L(\cos\theta). \qquad (1)$$

Here k is the wave number, σ_L the Coulomb phase shifts and $f_{\mathrm{R}}(\theta)$ is the usual Rutherford scattering amplitude given by

$$f_{\mathrm{R}}(\theta) = -\frac{\eta}{2k\sin^2(\theta/2)}\exp[2i\sigma_0 - i\eta\ln(\sin^2\frac{\theta}{2})], \qquad (2)$$

and the nuclear S-matrix elements S_L^N in this equation can be expressed by the nuclear phase shifts δ_L

$$S_L^N = \exp(2i\delta_L). \qquad (3)$$

In this work, we use the eikonal phase shifts based on the Coulomb trajectories of the colliding nuclei. If there is a single turning point in the radial Schrödinger equation, a first-order WKB expression for the nuclear elastic phase shifts δ_L, taking into account the deflection effect due to Coulomb field, can be written as [3,4]

$$\delta_L = \int_{r_t}^{\infty} k_L(r)\,dr - \int_{r_c}^{\infty} k_c(r)\,dr, \qquad (4)$$

where r_t and r_c are the turning points corresponding to the local wave numbers $k_L(r)$ and $k_c(r)$ given by

$$k_L(r) = k\Big[1 - \Big(\frac{2\eta}{kr} + \frac{(L+\frac{1}{2})^2}{k^2r^2} + \frac{U(r)}{E}\Big)\Big]^{1/2}, \qquad (5)$$

$$k_c(r) = k\Big[1 - \Big(\frac{2\eta}{kr} + \frac{(L+\frac{1}{2})^2}{k^2r^2}\Big)\Big]^{1/2}, \qquad (6)$$

where $U(r)$ the nuclear potential. If we consider the nuclear potential as a perturbation, the turning point r_t may be taken to be coincident with the distance of closest approach r_c given by

$$r_c = \frac{1}{k}\Big\{\eta + \Big[\eta^2 + (L+\frac{1}{2})^2\Big]^{1/2}\Big\}. \qquad (7)$$

Thus, the nuclear phase shift δ_L in Eq.(4) can be rewritten

$$\delta_L = -\frac{\mu}{\hbar^2}\int_{r_c}^{\infty}\frac{U(r)}{k_c(r)}dr - \frac{\mu}{2\hbar^4}\int_{r_c}^{\infty}\frac{U^2(r)}{k_c^3(r)}dr \qquad (8)$$

where $r = \sqrt{r_c^2 + z^2}$, μ is the reduced mass.

The first term in above equation is the ordinary Coulomb-modified eikonal phase shift function, while the second term is the first-order correction correspond to non-eikonal effects. The expressions of each terms in Eq.(8) are explicitly[11]

$$\delta_L^0(r_c) = -\frac{\mu}{\hbar^2 k}\int_0^{\infty} U(r)\,dz, \qquad (9)$$

$$\delta_L^1(r_c) = -\frac{\mu^2}{2\hbar^4 k^3}\Big(1 + r_c\frac{d}{dr_c}\Big)\int_0^{\infty} U^2(r)\,dz. \qquad (10)$$

The first-order eikonal correction term of the phase shift, $\delta_L^1(r_c)$ in Eqs. (10), can further be expressed as following

$$\delta_L^1(r_c) = -\frac{\mu^2}{\hbar^4 k^3}\int_0^{\infty}\Big[U^2(r) + rU(r)\frac{dU(r)}{dr}\Big]\,dz. \qquad (11)$$

The closed expression of the effective phase shift function including up to the first-order correction term may be written as

$$\delta_L(r_c) = -\frac{\mu}{\hbar^2 k}\int_0^{\infty} U_{\mathrm{eff}}(r)\,dz$$
$$= -\frac{1}{\hbar v}\int_0^{\infty} U_{\mathrm{eff}}(r)\,dz, \qquad (12)$$

where v is the relative velocity of the two scattering partners at infinity, and $U_{\mathrm{eff}}(r)$ is the effective optical potential given by

$$U_{\mathrm{eff}}(r) = U\Big\{1 + \frac{\mu}{\hbar^2 k^2}\Big[U + r\frac{dU}{dr}\Big]\Big\}. \qquad (13)$$

We can see that the phase shift calculation including non-eikonal corrections up to the first-order is equivalent to a zeroth-order calculation with effective potential $U_{\mathrm{eff}}(r)$.

In the semiclassical spirit, in order to assure the conservation of the angular momentum, one can change the asymptotic velocity that is used to calculate the nuclear eikonal

TABLE I: Parameters of the fitted Woods-Saxon potential for ^{16}O + ^{40}Ca and ^{16}O + ^{90}Zr systems at E_{lab} = 1503 MeV. Values are taken from Ref. [13].

System	V_0 (MeV)	r_v (fm)	a_v (fm)	W_0 (MeV)	r_w (fm)	a_w (fm)
^{16}O + ^{40}Ca	60.0	1.042	0.710	54.1	1.042	0.710
^{16}O + ^{90}Zr	129.0	0.946	0.790	124.1	0.946	0.790

TABLE II: χ^2/N values for ^{16}O + ^{40}Ca and ^{16}O + ^{90}Zr systems at E_{lab} = 1503 MeV by using the Coulomb-modified eikonal model based on asymptotic and tangential velocities at the distance of closest approach, respectively.

System	Asymptotic velocity		Tangential velocity	
	δ_0	$\delta_0 + \delta_1$	δ_0	$\delta_0 + \delta_1$
^{16}O + ^{40}Ca	5.22	3.08	4.31	2.63
^{16}O + ^{90}Zr	6.43	5.12	6.25	5.05

phase shift by the tangential velocity at the point of closest approach r_c [10],

$$v_c(b) = \frac{b}{r_c} v. \tag{14}$$

Then the Coulomb turning point correction in the eikonal phase shift of Eq.(12) takes the form

$$\delta_L(r_c) = -\frac{1}{\hbar v_c} \int_0^\infty U_{eff}(r) dz. \tag{15}$$

By taking $U(r)$ as the optical Woods-Saxon forms given by

$$U(r) = -\frac{V_0}{1 + e^{(r-R_v)/a_v}} - i\frac{W_0}{1 + e^{(r-R_w)/a_w}}, \tag{16}$$

with $R_{v,w} = r_{v,w}(A_1^{1/3} + A_2^{1/3})$, we can use the phase shift, Eq.(15), in the general expression for the elastic scattering amplitude given in Eq.(1).

III. RESULTS AND DISCUSSIONS

The elastic differential cross sections for ^{16}O + ^{40}Ca and ^{16}O + ^{90}Zr systems at E_{lab}

= 1503 MeV are calculated by using the first-order Coulomb-modified eikonal phase shift with the tangential velocity at the point of closest approach r_c. Parameters of the Woods-Saxon potential are given in Table I. The calculated results of the differential cross sections for the elastic scattering of ^{16}O + ^{40}Ca and ^{16}O + ^{90}Zr systems at E_{lab} = 1503 MeV are presented in Fig. 1 together with the observed data [13]. In this figure, the dashed and solid curves are the results using the tangential velocity for the zeroth-order eikonal phase shift and its first-order correction, respectively. As seen in this figure, there are the substantial differences between the dashed and solid curves when compared to the experimental data. Furthermore, these differences give some variations in the depths of the minimum and a change in the location of the minimum. As a whole, we can find in Fig. 1 that the two results calculated from the first-order correction improve the agreements with the observed data for ^{16}O + ^{40}Ca and ^{16}O + ^{90}Zr systems at E_{lab} = 1503 MeV compared to the results of the zeroth-order eikonal phase shifts.

TABLE III: Reaction cross sections for ^{16}O + ^{40}Ca and ^{16}O + ^{90}Zr systems at E_{lab} = 1503 MeV by using the Coulomb-modified eikonal model based on asymptotic and tangential velocities at the distance of closest approach, respectively. Values with the optical model are taken from Ref. [13].

System	Asymptotic velocity		Tangential velocity		Optical model
	δ_0	$\delta_0 + \delta_1$	δ_0	$\delta_0 + \delta_1$	
	(mb)	(mb)	(mb)	(mb)	(mb)
^{16}O + ^{40}Ca	1966	1980	1972	1986	1996
^{16}O + ^{90}Zr	2707	2722	2717	2731	2749

In order to investigate the tangential velocity effect to the differential cross sections at the distance of closest approach r_c, we present in Fig. 2(a)and 2(b) the cross sections using
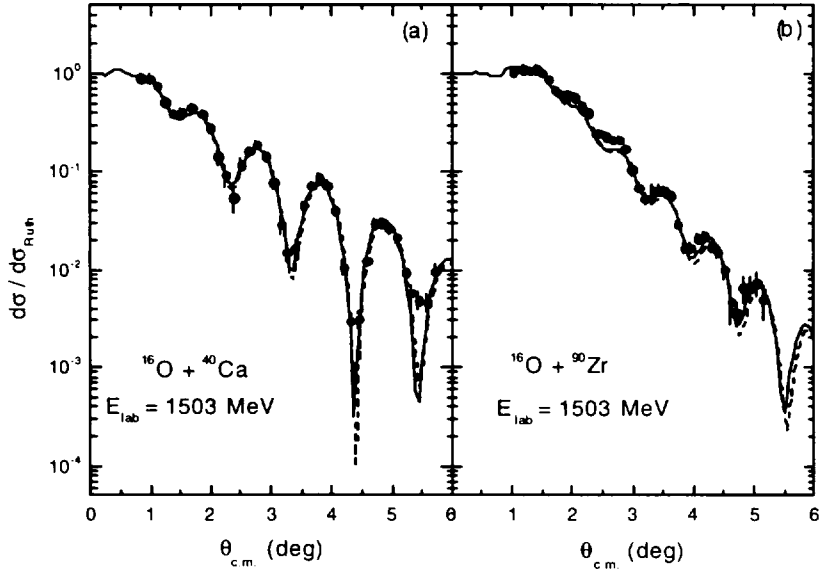

FIG. 1: Elastic scattering angular distributions for ^{16}O + ^{40}Ca and ^{16}O + ^{90}Zr systems at E_{lab} = 1503 MeV, respectively. The solid circles denote the observed data taken from Roussel-Chomaz et al. [13]. The dashed and solid curves are the calculated results by using the tangential velocity for zeroth- and first-order eikonal corrections, respectively.

the first-order Coulomb-modified eikonal model with the asymptotic and tangential velocities. In Fig.2(a) and 2(b), the dashed and solid curves are the calculated results from the asymptotic and tangential velocities, respectively. As seen in Fig. 2(a) and 2(b), the differences between the calculated results are small so that the dashed curves overlap with the solid curves. However, we can see in Table II that the values of χ^2/N for ^{16}O + ^{40}Ca and ^{16}O + ^{90}Zr systems at E_{lab} = 1503 MeV decrease in the calculated results with the tangential velocity compared to the ones with asymptotic one. As shown in table III,
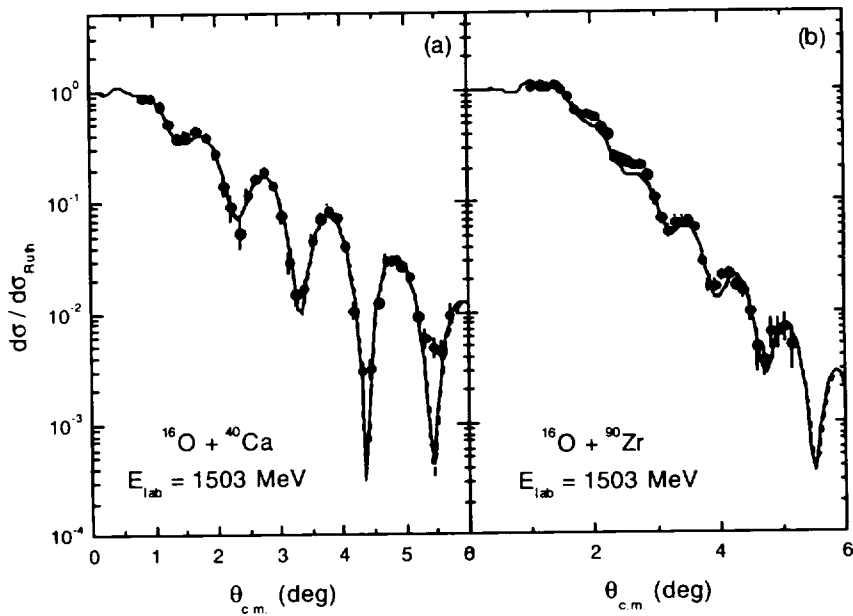

FIG. 2: Elastic scattering angular distributions for ^{16}O + ^{40}Ca and ^{16}O + ^{90}Zr systems at E_{lab} = 1503 MeV, respectively. The solid circles denote the observed data taken from Roussel-Chomaz et al. [13]. The dashed and solid curves are the first-order Coulomb-modified eikonal model calculations by using the asymptotic and tangential velocities, respectively.

the calculated results from the first-order corrected phase increase the reaction cross sections compared to ones of zeroth-order eikonal phase. Particularly, we can notice in this table that the agreements of the results from tangential velocity are satisfactorily good with the optical model results compared to the results of asymptotic velocity.

More insight into the diffractive and refractive phenomena can be provided by the representation of the elastic scattering amplitude in terms of the near-side and far-side components. The near- and far-side decompositions of the scattering amplitudes with the first-order Coulomb-modified eikonal model using the tangential velocity at r_c, for $^{16}O + ^{40}Ca$ and $^{16}O + ^{90}Zr$ systems at $E_{lab} = 1503$ MeV, were performed by following the Fuller's formalism [14]. The contributions of the near- and far-side components to the elastic scattering cross sections are shown in Fig. 3 along with the differential cross sections. The differential cross section is not just a sum of the near- and far-side cross sections but contains the interference between the near- and far-side amplitudes as shown in figure 3. The refractive oscillations observed in the angular distribution of the $^{16}O + ^{40}Ca$ system are due to the strong interference between the near-side and far-side components as shown in Fig. 3(a). Roussel-Chomaz et al. [13] have pointed out that such a behavior could be
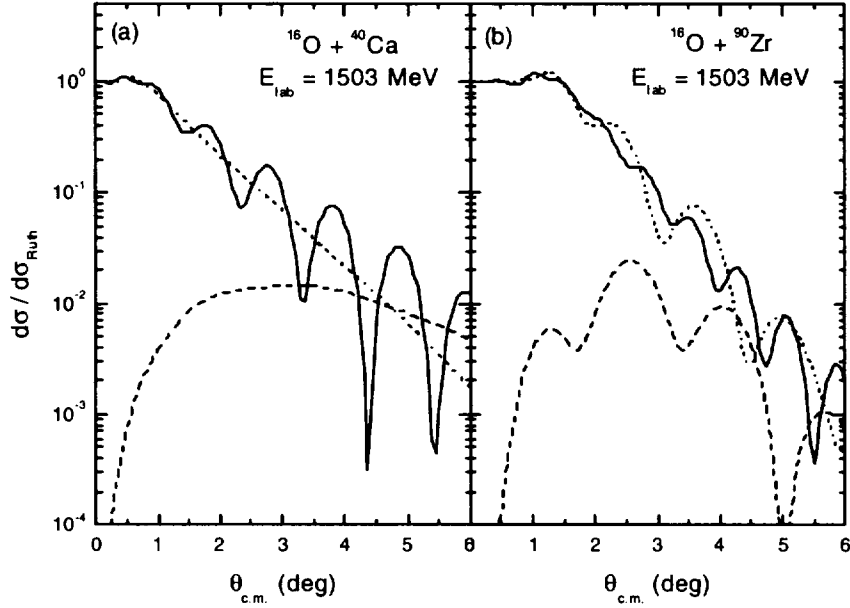

FIG. 3: Differential cross sections (solid curves), near-side contributions (dotted curves), and far-side contributions (dashed curves) following the Fuller's formalism [14] from the first-order Coulomb-modified eikonal model by using the tangential velocity.

qualitatively understood as a refractive phenomenon due to the attractive nature of the

potential. The near-side contributions dom-

inate for small angles and the far-side ones for large angles. The two contributions have equal magnitudes at $\theta = 4.7°$. On the other hand, in case of ^{16}O + ^{90}Zr elastic scattering, the far-side component becomes very small compared with the near-side one over the whole angle. Because of the smallness of the far-side amplitude, we can see that the cross sections of the ^{16}O + ^{90}Zr system show weak oscillations.

The transmission function $T_L = 1 - |S_L|^2$ is plotted versus the orbital angular momen-

tum in Fig. 4, along with the partial wave reaction cross section σ_L for ^{16}O + ^{40}Ca and ^{16}O + ^{90}Zr systems at $E_{lab} = 1503$ MeV, respectively. The transmission function can be explained using the imaginary part of the effective optical potential. As shown Fig. 4(a), the lower partial waves are totally absorbed and the T_L is decreased very rapidly in a narrow localized angular momenta zone. In
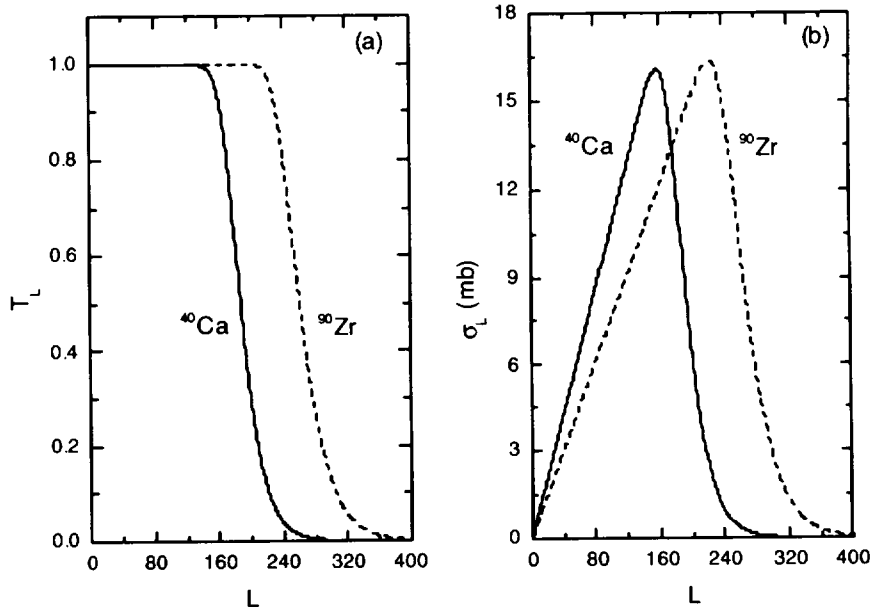

FIG. 4: (a) Transmission functions T_L and (b) Partial wave reaction cross sections σ_L for ^{16}O + ^{40}Ca and ^{16}O + ^{90}Zr systems at $E_{lab} = 1503$ MeV, respectively, plotted versus the orbital angular momentum L.

Fig.4(a), we can see that T_L of ^{16}O + ^{16}Zr is shifted toward the right compared with one

of ^{16}O + ^{40}Ca, as expected. Such shift is re-

flected in the reaction cross section, σ_R, as displayed in Table III, and indicate that the σ_R increases as the mass is heavier. We found in Fig. 4(b) that the values of the partial reaction cross section increase linearly up to L

= 157 for ^{16}O + ^{40}Ca and L = 223 for ^{16}O + ^{90}Zr, respectively. Beyond these L values, the partial reaction cross sections decrease quadratically.
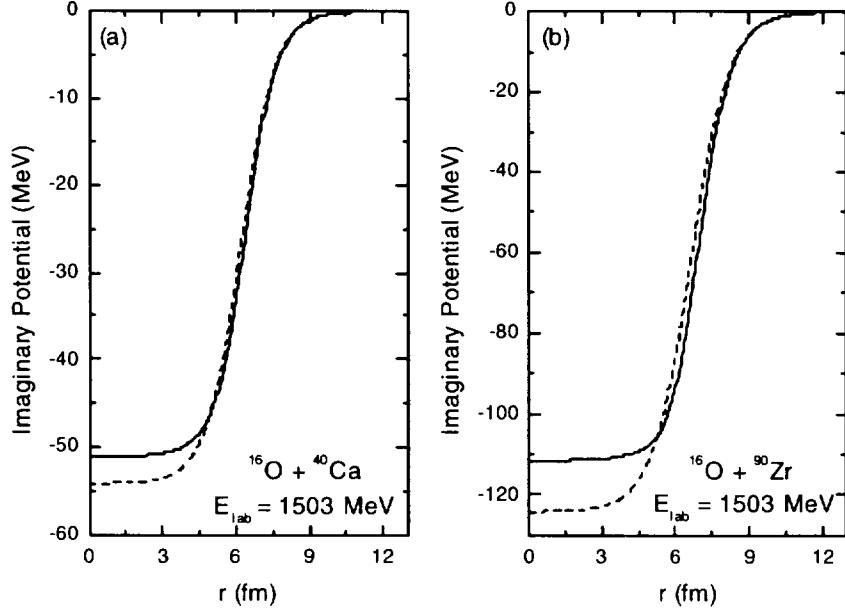

FIG. 5: Imaginary parts of effective potential for ^{16}O + ^{40}Ca and ^{16}O + ^{90}Zr systems at E_{lab} = 1503 MeV, respectively. The dashed and solid curves are the effective potentials for zeroth- and first-order eikonal corrections, respectively.

In figure 5, we plot the imaginary parts of effective potential in Eq.(13) and nominal potential in Eq.(16), and examine the effect of first-order non-eikonal correction. The solid curves are the first-order effective potentials $U_{eff}(r)$ given by Eq.(13), while the dashed curves are the nominal potential $U(r)$

given by Eq.(16). As shown in this figure, there is a difference between the two potentials. We can see in Eq.(13) that the effective imaginary potential with the first-order eikonal correction depends on the product of the real and imaginary potentials and their derivatives. Thus the depth of effective imag-

inary potentials are decreased in the central region. Also, the effective imaginary potentials are shifted to the right near the surface region. These differences at the central and surface region are mainly due to the correction term in Eq.(13). In the traditional optical model, it is assumed that the imaginary part of the potential is responsible for the absorption process in the nuclear reaction, and its shape should not be affected by the real part. The heavy-ion elastic scattering generally dominated by the strong absorption, which the implication that the data are only sensitive to the surface of the interaction region. Because of the shift to the right near the surface region, the reaction cross section in the first-order Coulomb-modified eikonal model have larger values compared to ones of the zeroth-order Coulomb-modified eikonal model.

IV. CONCLUDING REMARKS

In this study, we have analyzed the elastic scatterings of ^{16}O + ^{40}Ca and ^{16}O + ^{90}Zr systems at E_{lab} = 1503 MeV within the framework of the first-order Coulomb-modified eikonal model based on the tangential velocity at the point of closest approach r_c. We have found that the differential and reaction cross sections calculated from the first-order eikonal phase shifts improve the agreements with the experimental data and

optical model results for ^{16}O + ^{40}Ca and ^{16}O + ^{90}Zr systems at E_{lab} = 1503 MeV, respectively, compared to the results of the zeroth-order phases. In addition, the agreements between the calculated results with the tangential velocity, the experimental data and reaction cross sections, are improved comparing with the results with the asymptotic one.

Through near- and far-side decompositions of the elastic cross sections for ^{16}O + ^{40}Ca and ^{16}O + ^{90}Zr systems at E_{lab} = 1503 MeV, we have shown that the refractive oscillations of the ^{16}O + ^{40}Ca system are due to the strong interference between the near- and far-side amplitudes. However, in case of ^{16}O + ^{90}Zr system, the far-side component is very small compared with the near-side one, so that the cross sections show weak oscillations. The transmission function is shifted to the right, and the reaction cross section is increased as the target mass is heavier. The partial reaction cross sections increase linearly up to L = 157 for ^{16}O + ^{40}Ca and L = 223 for ^{16}O + ^{90}Zr, respectively. Beyond these L values, the partial reaction cross sections decrease quadratically. The effective imaginary potentials is shifted to the right near the surface regions compared to nominal potentials. These shift lead to some larger values on the reaction cross sections of the first-order Coulomb-modified eikonal model compared to ones in the zeroth-order Coulomb-modified eikonal model.

[1] T. W. Donnelly, J. Dubach and J. D. Walecka, Nucl. Phys. Nucl. Phys. **A232**, 355 (1974).

[2] J. Knoll and R. Schaeffer, Ann. Phys. (N.Y.) **97**, 307 (1976).

[3] C. K. Chan, P. Suebka and P. Lu P, Phys. Rev. C **24**, 2035 (1981).

[4] D. M. Brink, *Semi-Classical Methods for Nucleus-Nucleus Scattering* (Cambridge Univ. Press, Cambridge, 1985), p.37.

[5] R. da Silveira and Ch. Leclercq-Willain, J. Phys. G **13**, 149 (1987).

[6] G. Fäldt, A. Ingemarsson and J. Mahalanabis, Phys. Rev. C **46**, 1974 (1992).

[7] A. Ingemarsson and G. Fäldt, Phys. Rev. C **48**, R507 (1993).

[8] F. Carstoiu and R. J. Lombard, Phys. Rev. C **48** 830 (1993).

[9] S. M. Eliseev and K. M. Hanna, Phys. Rev. C **56**, 554 (1997).

[10] C. E. Aguiar, F. Zardi, and A. Vitturi, Phys. Rev. **C56**, 1511 (1997).

[11] M. H. Cha and Y. J. Kim, Phys. Rev. **C51**, 212 (1995).

[12] Y. J. Kim and M. H. Cha, Int. J. Mod. Phys. **E9**, 67 (2000).

[13] P. Roussel-Chomaz, N. Alamanos, F. Auger, J. Barrette, B. Berthier, B. Fernandez, and L. Papineau, Nucl. Phys. **A477**, 345 (1988).

[14] R. C. Fuller, Phys. Rev. C **12**, 1561 (1975).

E_{lab} = 1503 MeV 에서 ^{16}O 이온 탄성산란에 대한 제1차 쿨롱-수정된 Eikonal 모형 분석과 접선속도 보정

김 용 주

제주대학교 물리학과

최근접 거리에서 접선속도에 기초한 제1차 쿨롱-수정된 Eikonal 모형을 이용하여 E_{lab} = 1503 MeV 에서 ^{16}O + ^{40}Ca 와 ^{16}O + ^{90}Zr 계의 탄성산란을 분석하였다. 접선속도를 고려하여 계산한 미분단면적과 반응단면적은 점근속도를 고려한 계산결과들에 비해 실험데이터와 광학모형 결과들과 더 좋은 일치를 보여 주었다. 탄성산란단면적에 대한 근측과 원측 분해를 통하여 ^{16}O + ^{40}Ca 계의 진동구조는 근측과 원측 진폭들 사이의 강한 간섭현상에 기인하고 있고, ^{16}O + ^{90}Zr 계의 경우에는 근측 진폭이 지배적으로 기여함을 알 수 있었다.